PCGRIDDS-based isentropic analysis as a forecasting tool in the South African Weather Bureau

E de Coning
Weather Forecasting Research Programme, South African Weather Bureau, Private Bag X097, Pretoria 0001, South Africa

Abstract

The principles of isentropic analysis were introduced in the late 1930s, thus it is not a new concept. Although isentropic methods were used in the United States thereafter, they were abandoned due to several practical reasons that will be discussed in this paper. A revival of isentropic analysis took place in the 1970s due to certain corrections being made as well as the availability of computers to do the required conversion to isentropic co-ordinates in short periods of time. The main advantage of isentropic analysis is that it offers the ability to look at atmospheric motion in the way it actually happens - i.e., in three dimensions - due to the fact that isentropic surfaces follow the true motion of a parcel. This concept is especially important when moisture transport is evaluated since the "vertical" motion of the moisture is included in the graphical depiction on isentropic levels. Isentropic analysis of model output data is not meant as a substitute for isobaric analysis, but to complement it by offering a different and unique way to look at the data. In this paper the history and mathematical background of isentropic analysis are presented and then the common variables used in operational forecasting are defined together with their interpretation. A case study is presented where the conventional methods of forecasting missed the area where rain occurred, but isentropic analysis of the data clearly points towards the area where rain could have been anticipated. With the aid of PC-based software, the calculation of variables has become easy. Methods have also been developed to make the graphical depiction of isentropic variables easily accessible to an operational forecaster in South Africa. The operational use of isentropic analysis is recommended to supplement conventional methods used in forecasting offices around the country.

The history of isentropic analysis

Numerical weather prediction models usually provide a forecaster with output on pressure levels. Many a forecaster has, however, experienced difficulty describing moisture transport from one pressure level to the next due to the fact that atmospheric flow also has an adiabatic upward or downward component not depicted on the quasi-horizontal pressure levels. One way of overcoming this problem is through isentropic analysis where meteorological variables are depicted on levels of constant potential temperature, whose slope in many cases is identical to that of upward and downward trajectories followed by the air.

Potential temperature is defined as the temperature a parcel would have if it were transported without external energy gain or loss (i.e. adiabatically) to a pressure of 1 000 hPa. Hess (1959) showed that potential temperature is related to entropy (a measure of disorder expressed in $J \cdot kg^{-1}$) and by this relationship it followed that a parcel that ascends under dry adiabatic conditions conserves its potential temperature and also its entropy. Operationally meteorologists use the terminology 'isentropic' surface to refer to a level of constant potential temperature.

Isentropic analysis was first addressed by meteorologists such as Rossby et al. (1937) and Namias (1938). The former author argued that for synoptic time scales, parcels of air are thermodynamically bound to their isentropic surfaces in the absence of diabatic processes. Since the flow of air in the atmosphere is three-dimensional and not fragmentary (as depicted on isobaric surfaces), Rossby et al. (1937) were of the opinion that "*it can hardly be doubted that the isentropic charts represent the true motion of air more faithfully by far than synoptic charts for any fixed level in the free atmosphere*".

* To whom all correspondence should be addressed.
☎(012) 309-3081;fax (012) 323-4518 e-mail: estelle@cirrus.sawb.gov.za
Received 2 August 1999; accepted in revised form 12 April 2000.

Analysis by means of isentropic co-ordinates was used by the United States' Weather Service in the late 1930s, but it was later discontinued due to the following reasons (Bleck, 1973 and Wilson, 1985):

- Standardisation took place during the 2nd World War and the aviation community required winds on constant pressure levels.
- Fast computers were not available at the time to perform the computations within operational time constraints.
- The Montgomery Stream function was initially calculated incorrectly; this was later rectified by Danielsen (1959).

The availability of computers in the 1970s together with Danielsen's correction created new opportunities for meteorologists to do analyses on isentropic levels, for research and operational forecasting.

Some recent studies done with isentropic analysis include work on:

- cut-off lows (Mills and Boa-Jun, 1995);
- elevated thunderstorms with heavy rainfall (Market and Moore, 1995);
- snow (Nolan and Moore, 1995);
- heavy rainfall over South Africa in 1996 (De Coning et al., 1998); and
- severe convection in South Africa (De Coning and Petersen, 1999).

Mathematical background to isentropic analysis

Following Hess (1959), potential temperature is defined as:

$$\theta = T\left(\frac{1000}{p}\right)^{\kappa}$$

where $\kappa = R/C_p$, which is referred to as Poisson's equation for potential temperature. The potential temperature, θ, is physically defined as the temperature that a parcel of air would have if it were compressed (or expanded) adiabatically from its original pressure to 1 000 hPa.

In the troposphere the atmosphere is on average stable, thus:

$$\frac{-\partial T}{\partial Z} = \gamma_{envir} < 9.5\,^{o}C\,km^{-1}$$

In such an atmosphere the potential temperature increases with height:

$$\frac{1}{\theta}\frac{\partial \theta}{\partial z} = \frac{\Gamma_d - \gamma}{T}$$

where:

Γ_d is the dry adiabatic lapse rate and
γ is the environmental lapse rate.

If the atmosphere is stable then:

$\gamma < \Gamma_d$, and $\partial\theta/\partial Z > 0$ which means that θ increases with height.

If the lapse rate is neutral then:

$\gamma = \Gamma_d$, and $\partial\theta/\partial Z = 0$ which means that θ is constant with height,

and if the lapse rate is superadiabatic, then:

$\gamma > \Gamma_d$, and $\partial\theta/\partial Z < 0$ which means that θ decreases with height (Rogers and Yau, 1989).

Potential temperature increases equatorward at about the same rate as the dry bulb temperature. So the troposphere may be viewed as being composed of a number of isentropic layers which gradually descend from cold polar to warmer subtropical latitudes. As one ascends from the troposphere into the stable stratosphere isentropic surfaces become compacted with height. This attribute makes isentropic surfaces extremely valuable for resolving upper-level stable frontal zones in the presence of upper tropospheric wind maxima or jet streams. Thus, *in a stably stratified atmosphere potential temperature can be an excellent vertical co-ordinate - provided that it increases progressively with height everywhere - thereby avoiding the difficulties of dealing with a vertical coordinate (like pressure) which decreases with height* (Moore, 1992). Also, isentropic surfaces tend to run parallel to frontal zones as opposed to pressure surfaces which cut through the frontal zones.

Potential temperature is a conservative property for parcels of air under adiabatic conditions (no changes in heat due to processes such as radiation, mixing with environmental air and latent heating/evaporative cooling). These restrictions would seem to make the application of this thermodynamic variable very limited. However, diabatic heating and cooling processes are usually secondary in importance for temporal scales on the order of the synoptic ($\pm$ 1 d) scale. It can be shown that the entropy (ϕ) of an air parcel is related to its potential temperature as:

$$\phi = C_p \ln\theta + constant$$

Therefore a parcel which ascends under dry adiabatic conditions conserves its potential temperature and also its entropy. A layer of air in which **potential temperature is constant**, is described as an **equal entropy or isentropic layer**. Entropy is defined as a measure of the disorder of a system and is expressed in units of $J \cdot kg^{-1}$. Operational meteorologists have little use for this rather mystical concept and aside from using the term isentropic, potential temperature is the preferred variable rather than entropy.

Advantages and disadvantages of isentropic analysis

The advantages of isentropic analysis have been described by various authors; a summary of the advantages includes:

- Isentropic flow presents a truer picture of the three-dimensional air motion than isobaric surfaces (Carlson, 1991). Uccellini (1995) stated that isentropic analysis is the optimal way to represent a three-dimensional flow region onto a two-dimensional "horizontal" surface.
- For synoptic time scales air parcels are thermodynamically bound to their isentropic surfaces in the absence of diabatic processes (Rossby et al., 1937), i.e. the parcels will stay on their respective isentropic levels.
- Isentropic analysis provides an easy way to compute vertical motion directly, since "horizontal" flow along the isentropic surfaces includes the adiabatic component of the vertical motions (Danielsen, 1961; Uccellini, 1995).
- A more continuous moisture field is depicted on isentropic surfaces than on isobaric surfaces (Oliver and Oliver, 1951). Uccellini (1995) stated that isentropic analysis is the most accurate way for analysing and predicting moisture fields, moisture transports and associated precipitation.
- As a first approximation the atmospheric motion is adiabatic (as much as it is geostrophic) and this motion is related to the configuration and origin of air streams. Isentropic analysis can be used to distinguish between airstreams from different origins (Carlson, 1991).

It is important to know the disadvantages of isentropic analyses, which include:

- Choosing the proper isentropic surface to work with (Moore, 1992) is not as obvious as in isobaric analysis (i.e. always working with 850 hPa or 500 hPa). For a representation at the surface, it is important to choose a level which is close to the surface (display together with topography), but does not intersect the ground or is underneath the ground. This can be done by means of displaying potential temperature (θ) on the surface **or** by looking at potential temperature on a vertical cross section where topography is also indicated. Similar displays can be used to see which isentropic level is representative of the middle and upper troposphere.
- The "inertia" problem (Wilson, 1985); namely that weather forecasters still "think in pressure co-ordinates".

Forecasters should, however, familiarise themselves with isentropic analysis, since "*in many cases isentropic analyses should result in a better understanding of the atmosphere and better short range forecasts*" (Anderson, 1984) and weather systems and air flow are, after all, three-dimensional.

Isentropic variables and their interpretation

Static instability or isentropic mass within the layer

The mass within an isentropic layer is represented by the pressure depth of the layer (Δp) which also indicates the static stability of the layer (Petersen and Korotky, 1999):

$$\Delta p = p_b - p_t$$

where *t* and *b* refer to top and the bottom of the layer, respectively.

Δp is then always positive because pressure decreases with height as long as potential temperature increases with height, which is usually the case.

Thus, areas where the layer is thick (typically warm sector regions) indicate less stability and greater mass, while thin layers (typically in frontal zones) depict more stable regions, and correspondingly less mass (Petersen and Korotky, 1999).

Adiabatic vertical motion

Analysis of wind **V** and pressure p on an isentropic surface can yield a direct, quantitative estimate of the vertical velocity (omega) simply from the expansion of the total derivative (dp/dt) where:

$$\omega = \frac{dp}{dt} = \underbrace{\frac{\partial p}{\partial t}}_{1} + \underbrace{\bar{V} \bullet \bar{\nabla}_{\theta} p}_{2} + \underbrace{\frac{\partial p}{\partial \theta}\frac{d\theta}{dt}}_{3}$$

The first term is the local pressure change, the second term is pressure advection and the third term represents the contribution to vertical motion by diabatic processes.

When Term 3 is non-zero, it forces the parcel to "jump" off the isentropic surface. In a stable atmosphere $\partial P/\partial \theta$ is negative because θ increases as P decreases. The sign of Term 3 thus depends totally on the sign of the diabatic term, $d\theta/dt$; which is positive for heating and negative for cooling. Thus, diabatic heating (cooling) will cause upward (downward) motion with respect to the isentropic surface. Measuring $d\theta/dt$ is not easy, but fortunately in synoptic scales of motion and pre-severe storm environments it plays a less important role in the changes of ω (Moore, 1992).

Usually the pressure advection (Term 2) yields an acceptable approximation to adiabatic vertical motion much of the time, because diabatic processes (Term 3) tend to offset local pressure tendencies in Term 1 (Korotky et al. 1999). When the air is saturated, Term 3 would amplify the vertical motion (as latent heat would take the parcel up and off the isentropic surface), but this effect would be compensated by increases in Term 1 as the isentropic surface would descend when heated diabatically (Moore, 1992).

There are situations, however, where the damping effect of diabatic processes are insufficient to cancel the contribution from large, local pressure changes (as shown by Korotky et al., 1999) or within a convective situation (Moore, 1986) or when substantial snow falls (10 to 50 cm) were recorded (Market et al., 1999).

In the current case, however, no extreme weather event occurred and no major changes in the pressure patterns were evident. Therefore, the adiabatic vertical motion was approximated using only Term 2:

$$\omega \approx \bar{V} \bullet \bar{\nabla}_{\theta} p$$

Condensation pressure (p_c) difference

Condensation pressure is defined as the pressure to which a parcel of unsaturated air must be elevated dry-adiabatically in order to reach saturation, i.e. the condensation level. It was recommended that the condensation pressure should be used for isentropic analysis. It can be expressed as (Byers, 1938):

$$p_c = p\left(\frac{T_c}{T}\right)^{\frac{C_p}{R_d}}$$

where:

T is the temperature at a point with pressure p ($>p_c$) on the isentropic surface;

T_c is the temperature at p_c (isentropic-condensation temperature);

m is the molecular weight of dry air;

C_p is the specific heat at constant pressure and R_d is the dry gas constant.

The condensation level is defined as the level at which a parcel of moist air becomes saturated when it is displaced vertically and adiabatically.

The key advantage of condensation pressure over specific humidity q, is that condensation pressure represents moisture differences better at low values of q.

Another variable, namely condensation pressure difference, is also useful to present moisture values in isentropic analysis. This variable is computed by subtracting the value of condensation pressure from the corresponding pressure value. The smaller the value of the condensation difference, the closer to saturation a parcel is (Anderson 1984).

This variable is useful for the forecasting of fog where the moisture is only spread over a shallow layer of the atmosphere.

Moisture flux convergence/divergence on a certain level

On an isentropic surface or LEVEL, the **moisture flux** is computed as the product of the moisture and the wind (qV). **Moisture flux convergence** is calculated by taking the negative of the divergence of the moisture transport/flux field (Petersen and Korotky, 1999):

$$-\bar{\nabla} \bullet (q\bar{V}) = -\bar{V} \bullet \bar{\nabla} q - q\bar{\nabla} \bullet \bar{V}$$

Moisture flux convergence/divergence measures both the advection of the moisture along an isentropic surface and the destabilisation/stabilisation associated with the convergence/divergence of air on the surface. Convergence/divergence results in spreading/contracting of the isentropic surfaces above and below the surface where the moisture flux divergence was calculated (Petersen and Korotky, 1999).

Moisture stability flux divergence in a layer

The total quantity (i.e. volume) of moisture contained within a LAYER bounded by two isentropic surfaces is a function of the mean moisture (q) in the layer, and the mass which holds the moisture. Therefore the total moisture content of the LAYER is represented by the product of the mean moisture and the pressure depth of the LAYER ($q\Delta p$).

Calculating the product of ($q\Delta p$) and the wind i.e. ($q\Delta p$)**V**, will give the moisture flux (or transport of moisture) in the LAYER.

Since the moisture and mass within an isentropic layer vary horizontally, the total moisture field locates the greatest mass per unit area of moisture in the layer. A more direct measure of moisture transport and moisture flux convergence can be computed by incorporating the mass (and thus the total moisture) within an isentropic layer (Petersen and Korotky, 1999):

$$-\bar{\nabla} \bullet \left[\left(\bar{q}\Delta p\right)\bar{\bar{V}}\right] = -\bar{\bar{V}} \bullet \bar{\nabla}\left(\bar{q}\Delta p\right) - \left(\bar{q}\Delta p\right)\bar{\nabla} \bullet \bar{\bar{V}}$$

This quantity (moisture stability flux convergence) measures both the advection of layer total moisture and the convergence field acting on the layer total moisture. Convergence of this field indicates where moisture is increasing locally in conjunction with

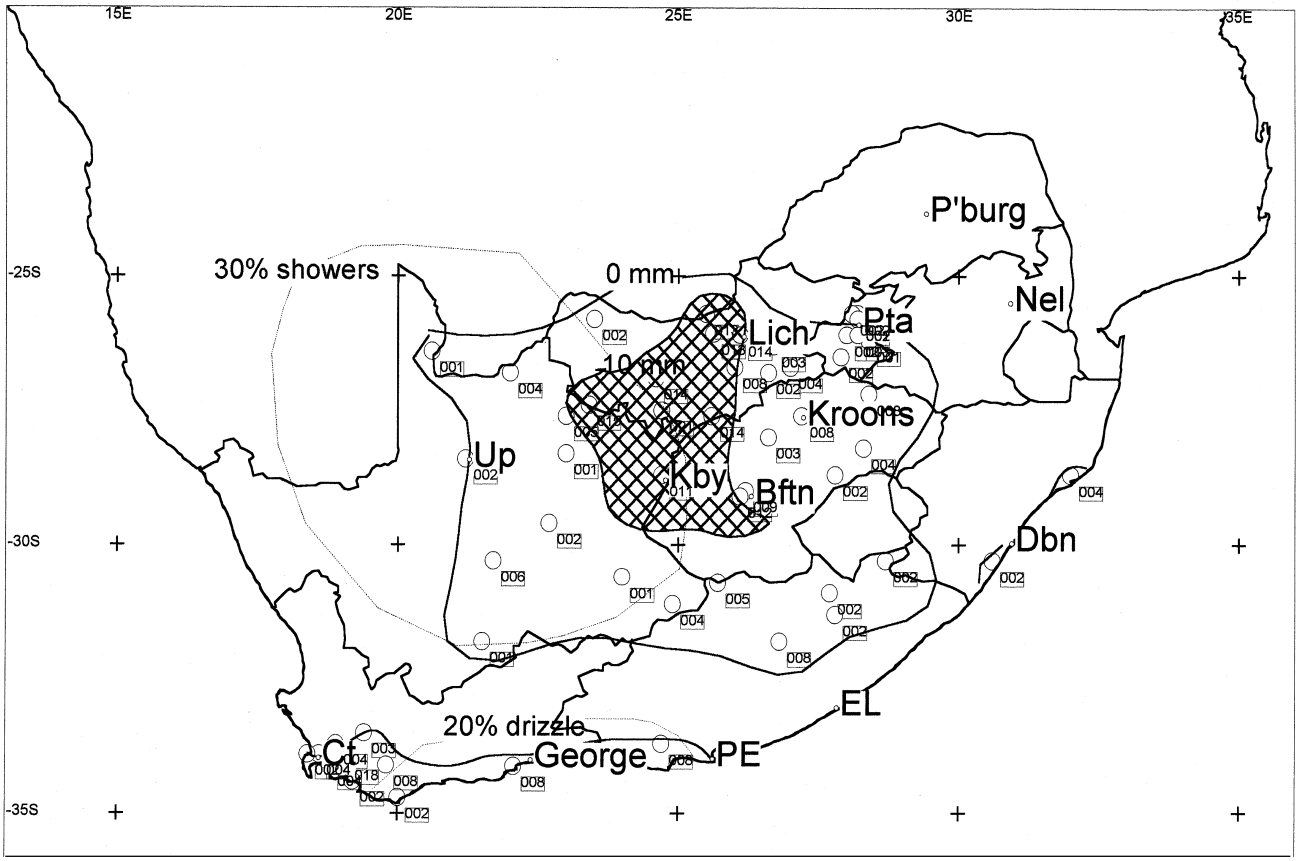

Figure 1
Reported rainfall (mm) for 14 May 1999 (solid lines) and forecasted rainfall (dotted lines). Area where falls were more than 10 mm is hatched.

decreasing stability, thus indicating where low-level processes are focusing the greatest convective potential (Petersen and Korotky, 1999).

Case study: 14 May 1999

Reported rainfall

Aerial extent

Rain fell over a large area of the central interior of the country (Fig. 1) on 14 May 1999. Due to the passing of a cold front, small amounts of precipitation were also recorded along the Cape South coast. Most of the rainfall totals were less than 10 mm, but heavier amounts were reported over the western half of the Free State, the eastern parts of Northern Cape and the south-western parts of the North-West Province. Some of the stations which reported more than 10 mm (in the 24 h period ending at 08:00 on the 15th) can be seen in Table 1.

Time distribution

Light rainfall was recorded from 19:00 UTC (universal time constant) until 21:00 UTC on the 14th over virtually the entire area described above. There was, however, a second rainfall event which occurred after 00:00 UTC on the 15th. This persisted until approximately midday on the 15th with more significant amounts recorded. This episode mainly influenced the western half of the Free State, the eastern parts of Northern Cape and the south-western parts of the North-West Province. This event also constituted the bulk of the rainfall recorded at the above-mentioned stations.

TABLE 1
RAINFALL REPORTS MORE THAN 20 mm

Place	Rainfall (mm)
Bloemhof	20.8
Armoedsvlakte	13.5
Schweizer-Reneke	17.0
Kuruman	14.6
Hertzogville	11.0
Kimberley	17.5
Bloemfontein (Zoo)	12.0
Reddersburg	16.0
Barkly West	14.5
Griekwastad	11.5
Verkeerdevlei	16.0
Magogong	16.5

Isobaric perspective

For the purpose of this study the local version of the Eta model was used which has a horizontal resolution of 48 km and 38 levels in the vertical.

850 Heights

At 12:00 UTC (12 h forecast; Fig. 2a) there was a high over the north-eastern part of the country, a low was on the Cape south coast from which a cold front extended north-westwards, and a warm

front north-eastwards. Signs of a disturbance were evident over southern Namibia. At 18:00 UTC (18 h forecast; Fig. 2b) the low pressure system had moved slightly eastward with a secondary low developing over the north-western Cape interior. The cold front was still extending to the north-west and the warm front was aligned with the east coast. The disturbance over Namibia has deepened and moved eastward over the Kalahari ahead of the front. By 24:00 UTC (24-h forecast; Fig. 2c) the low had advanced south-eastward well off the continent, while the secondary trough was nearly stationary. The disturbance over the Kalahari had now formed a closed low and had moved into the south-western parts of the North-West Province.

500 hPa Heights

At 12:00 UTC (12 h forecast; Fig. 3a) a fairly shallow trough was evident to the south-west of the country, highlighting the baroclinicity of the system. Far ahead of this trough (approx. 28°E) a perturbation was discernable over the north-eastern interior. By 18:00 UTC (18h forecast; Fig. 3b) the trough in the south-west had deepened slightly as it approached the south-west coast. The perturbation to the north-east was weakening with signs of a second perturbation developing over south-eastern Namibia. At 24:00 UTC (24 h forecast; Fig. 3c) the trough had further deepened in the south-west while moving little. The first perturbation was then east of 30°E, while the second was ever so slightly visible over the central interior.

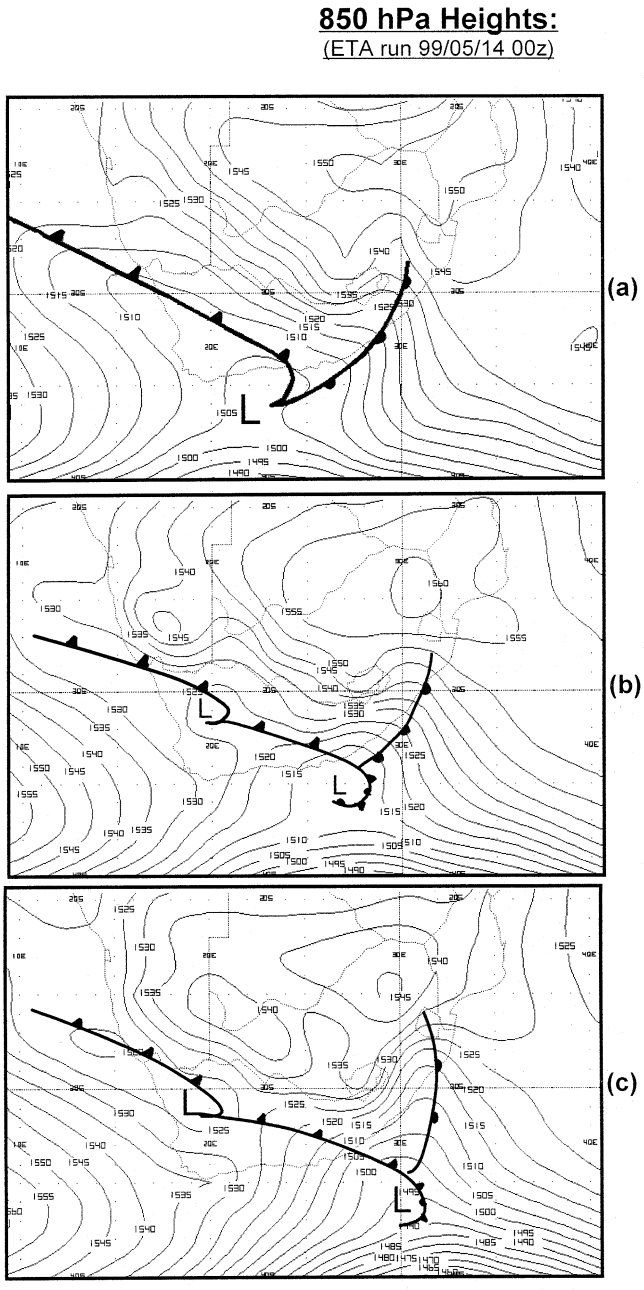

Figure 2
850 hPa heights (gpm: geopotential metres) from the Eta model's midnight run (99051400) for a) 12:00 UTC, b) 18:00 UTC and c) 24:00 UTC

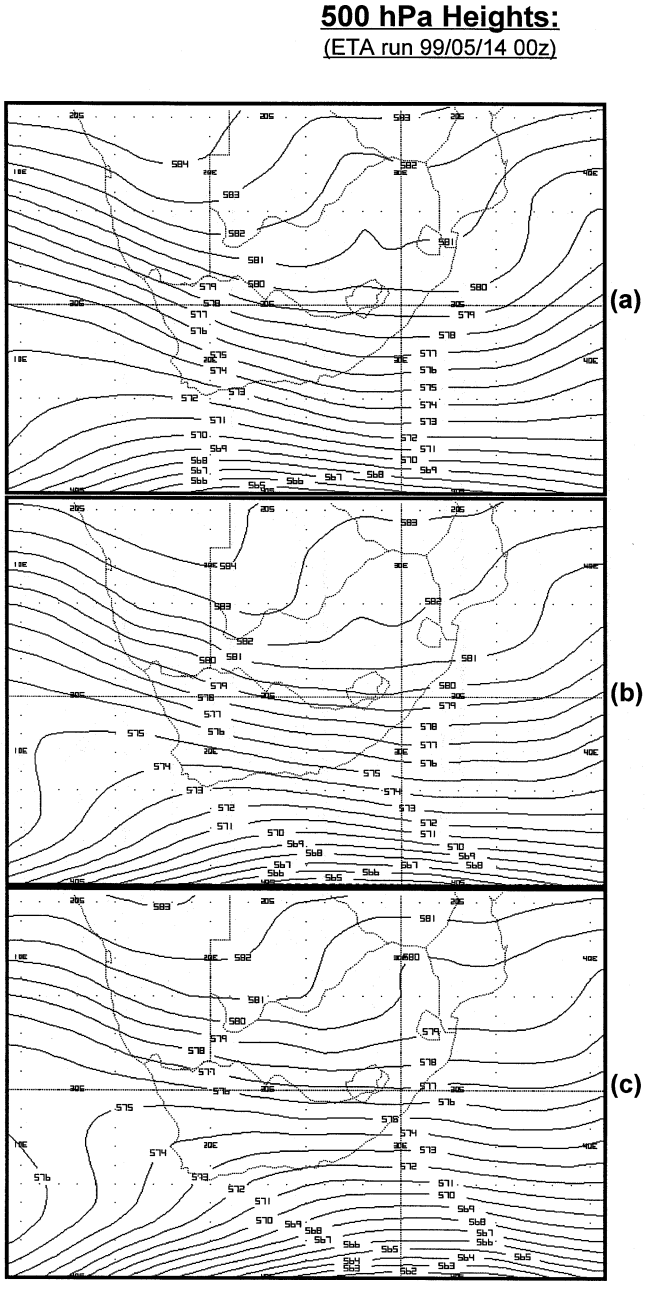

Figure 3
500 hPa heights (x10 gpm) from the Eta model's midnight run (99051400) for a) 12:00 UTC, b) 18:00 UTC and c) 24:00 UTC

500 hPa temperatures

At 12:00 UTC (Fig. 4a) the lowest temperatures (-16°C) were over the western Cape, while thermal troughs (areas where temperatures were lower than in the vicinity) were evident over the Northern Cape and along the eastern escarpment. By 18:00 UTC (Fig. 4b) it had cooled down to -18°C over the southern Cape, with the thermal trough over the northern Cape having progressed eastwards. The thermal trough over the escarpment had weakened somewhat. Temperatures over the southern Cape didn't change much by 24:00 UTC (Fig. 4c), but a clearly defined thermal trough had developed along the west coast. The thermal trough over the central interior had deepened significantly.

700 hPa vertical velocity (T)

At 12:00 UTC (Fig. 5a) there was a large area of weak upward motion (negative values) across the country, except over the south-east coast. By 18:00 UTC (Fig. 5b) the upward motion was largely confined to the interior and by 24:00 UTC (Fig. 5c) there was a region of downward motion behind the perturbations (over southern Namibia and Northern Cape). Aside from that, upward motion was concentrated in a band stretching north-west to south-east over the central parts of the country.

850 hPa specific humidity

The specific humidity fields revealed a concentration of moisture over the central and eastern interior as well as northern Namibia for

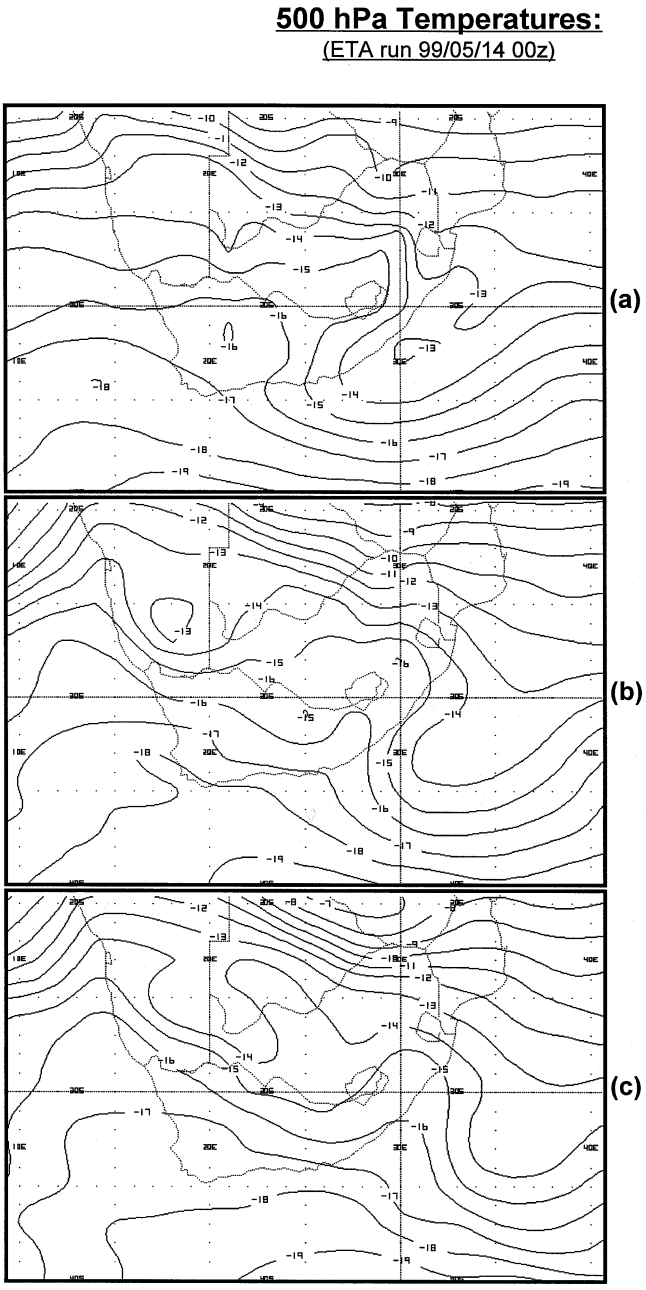

Figure 4
500 hPa temperatures (°C) from the Eta model's midnight run (99051400) for a) 12:00 UTC, b) 18:00 UTC and c) 24:00 UTC

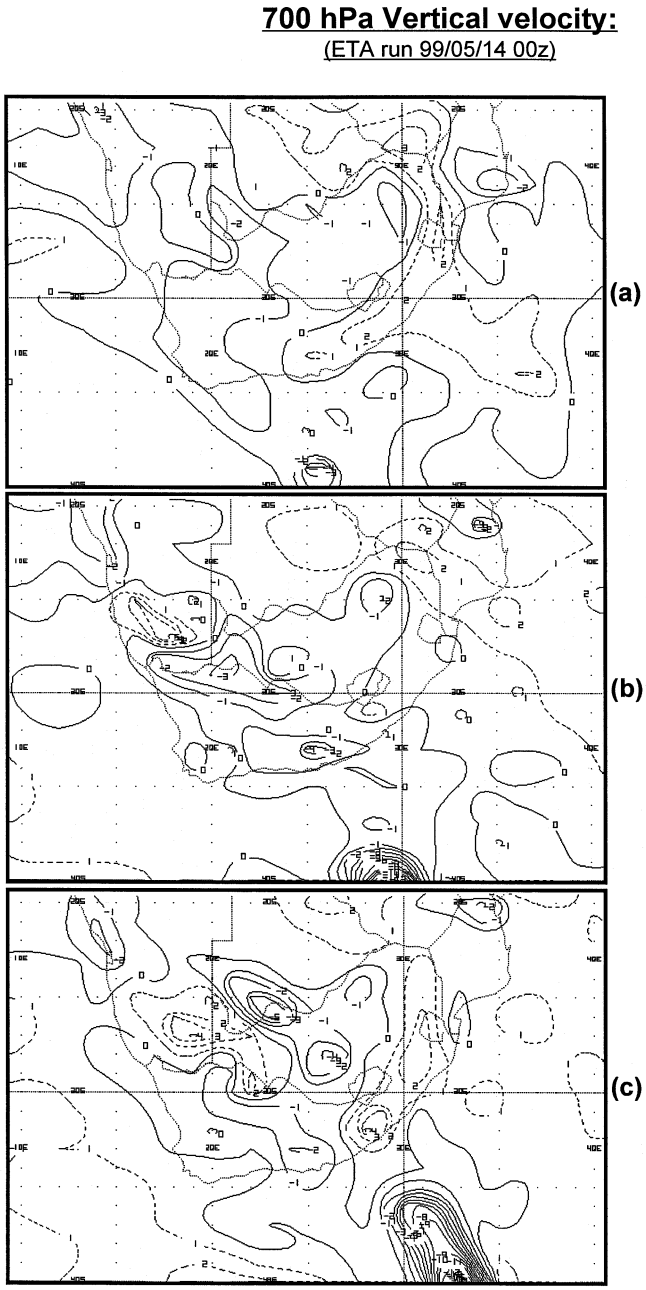

Figure 5
700 hPa vertical velocity (Pa s^{-1})from the Eta model's midnight run (99051400) for a) 12:00 UTC, b) 18:00 UTC and c) 24:00 UTC

the entire period (Fig. 6a-c). However, by 24:00 UTC these two areas were linked by a band of moisture across the Kalahari.

Isobaric interpretation

The forecast issued by Central Forecasting Office (in Pretoria) for the 14th made mention of moisture flux convergence in the lower layers combined with vertical motion over the eastern parts of the country, south-eastern Namibia and south-western Botswana. Later in the forecasting period increased uplift of moist air was expected together with upper-level divergence. The forecast thus indicated that isolated showers with a 30% probability would occur over southern Namibia and the western parts of the Free State spreading to the northern parts of the south-eastern Cape later. A 20% chance of drizzle along the Cape south coast was also expected (See dotted lines in Fig. 1).

Isentropic perspective

Chosen levels and layers

The nature of isentropic analysis requires that potential temperature levels and/or layers are chosen near the surface but do not intersect with the surface. From this it stems that the levels and layers need to be chosen carefully and also in conjunction with the

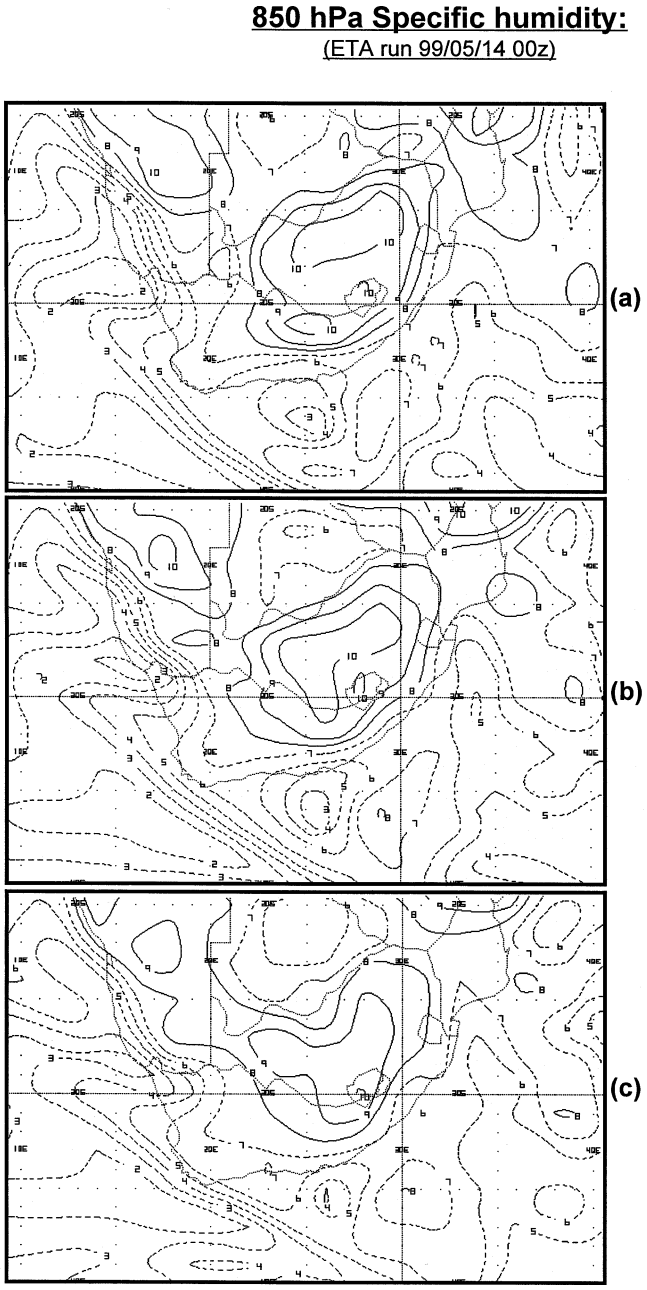

Figure 6
850 hPa specific humidity (g·kg^{-1}) from the Eta model's midnight run (99051400) for a) 12:00 UTC, b) 18:00 UTC and c) 24:00 UTC

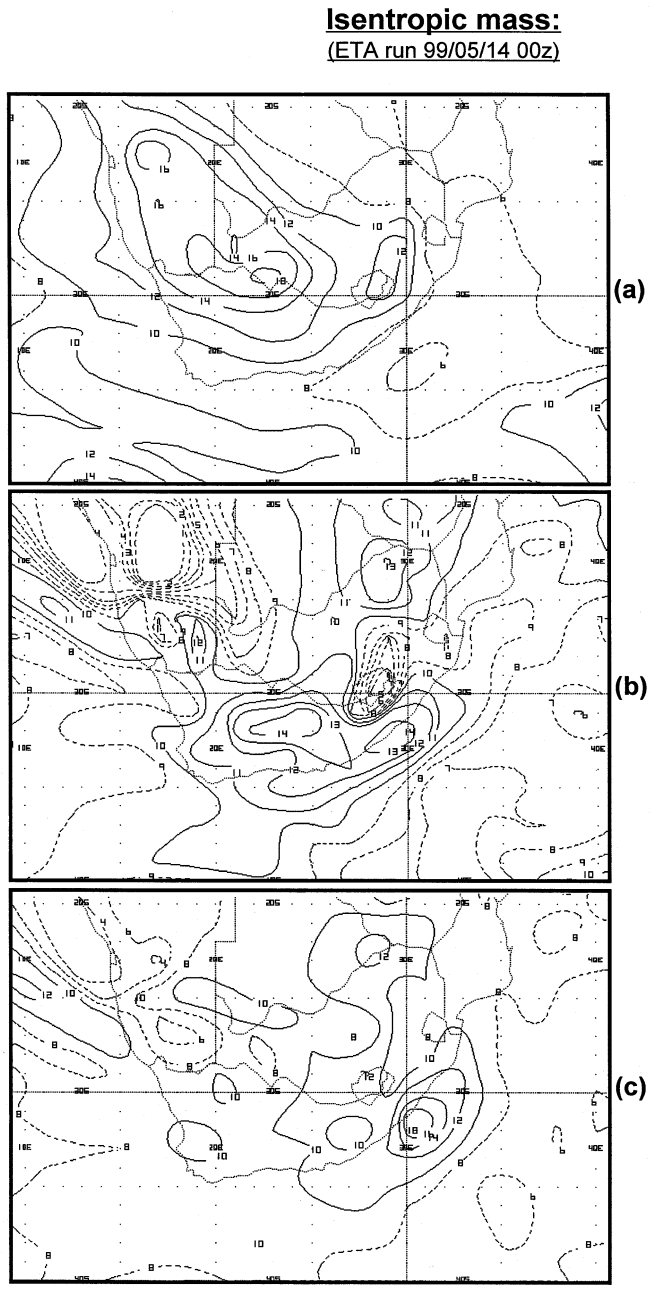

Figure 7
Isentropic mass (x10 hPa) from the Eta model's midnight run (99051400) for a) 12:00 UTC in the 310-314K layer, b) 18:00 UTC in the 302-306K layer and c) 24:00 UTC in the 302-306K layer

diurnal change in surface potential temperature. For this case the following were chosen:

TABLE 2
Forecast Hours, Layers and Levels for this Study

Forecast hour	Level	Layer
12	310K	310-314K
18	302K	302-306K
24	302K	302-306K

Isentropic mass

Isentropic mass is an indicator of static stability. Higher (Lower) values mean less (more) stable air.

At 12:00 UTC (Fig. 7a) the maximum isentropic mass corresponds with the warm sector between the cold and warm fronts described in the isobaric perspective. Thus, this region (over the central interior) was the least stable. By 18:00 UTC (Fig. 7b) more stable air invaded this area of instability from the north-west as well as from the east, leaving the a narrow corridor of unstable air extending from the southern parts of the country northward over the central interior. Six hours later (Fig. 7c) the stable air which originated in the north-west extended southward and influenced

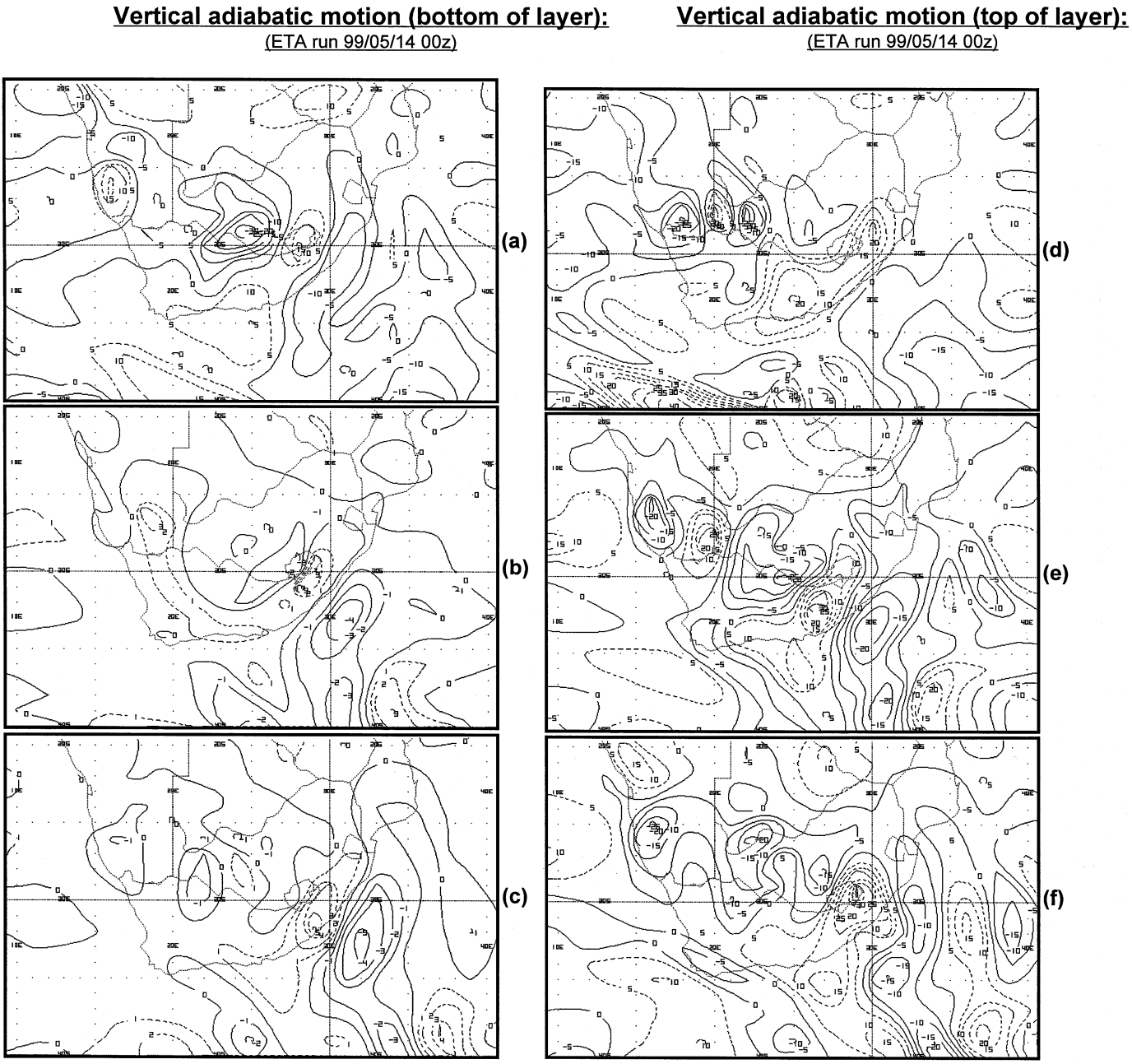

Figure 8

Vertical adiabatic motion (10^{-3} hPa·s^{-1}) from the Eta model's midnight run (99051400) for the bottom of the layer at a) 12:00 UTC at 310K, b) 18:00 UTC at 302K and c) 24:00 UTC at 302K and for the top of the layer at d) 12:00 UTC at 314K, e) 18:00 UTC at 306K and f) 24:00 UTC at 306K

the western half of the country, while less stable air (greater mass) dominated the central and eastern parts.

Vertical adiabatic motion (calculated as approximated earlier)

Bottom of layer

Upward motion (negative values) dominated the central part of the country at 12:00 UTC (Fig. 8a). It weakened somewhat by 18:00 UTC (Fig. 8b), but was still concentrated over the central parts of the country. Stronger downward motion occurred over the western parts. The area of upward motion was divided in half at 24:00 UTC (Fig. 8c) by weak downward motion over the eastern parts of the Northern Cape, with a re-intensification of upward motion to the west of this area.

Top of layer

The area of upward motion at 12:00 UTC (Fig. 8d) was 4° west of the location at the bottom of the layer and also extended to the west coast. By 18:00 UTC (Fig. 8e) the area of upward motion was similar to the area of upward motion at the bottom of the layer, albeit more pronounced. At 24:00 UTC (Fig. 8f) the vertical adiabatic motion was significantly stronger than at the bottom layer.

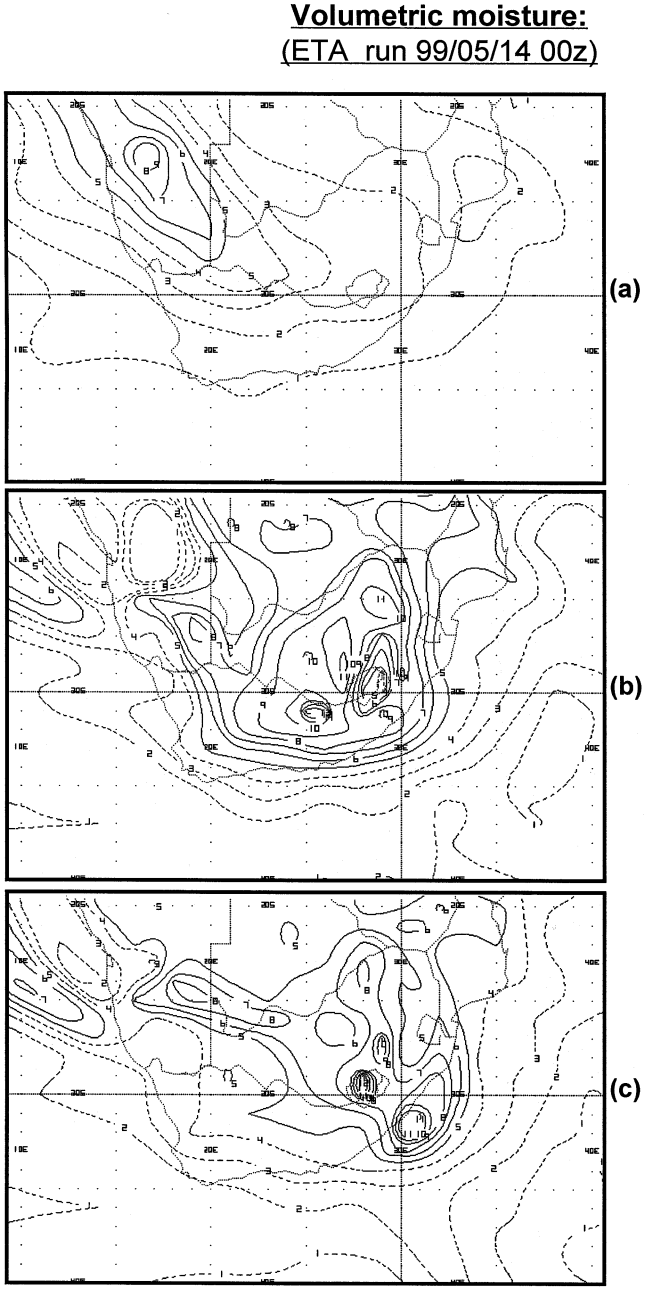

Figure 9

Volumetric moisture (10^{-1} g·cm^{-2}) from the Eta model's midnight run (99051400) for a) 12:00 UTC in the 310-314K layer, b) 18:00 UTC in the 302-306K layer and c) 24:00 UTC in the 302-306K layer

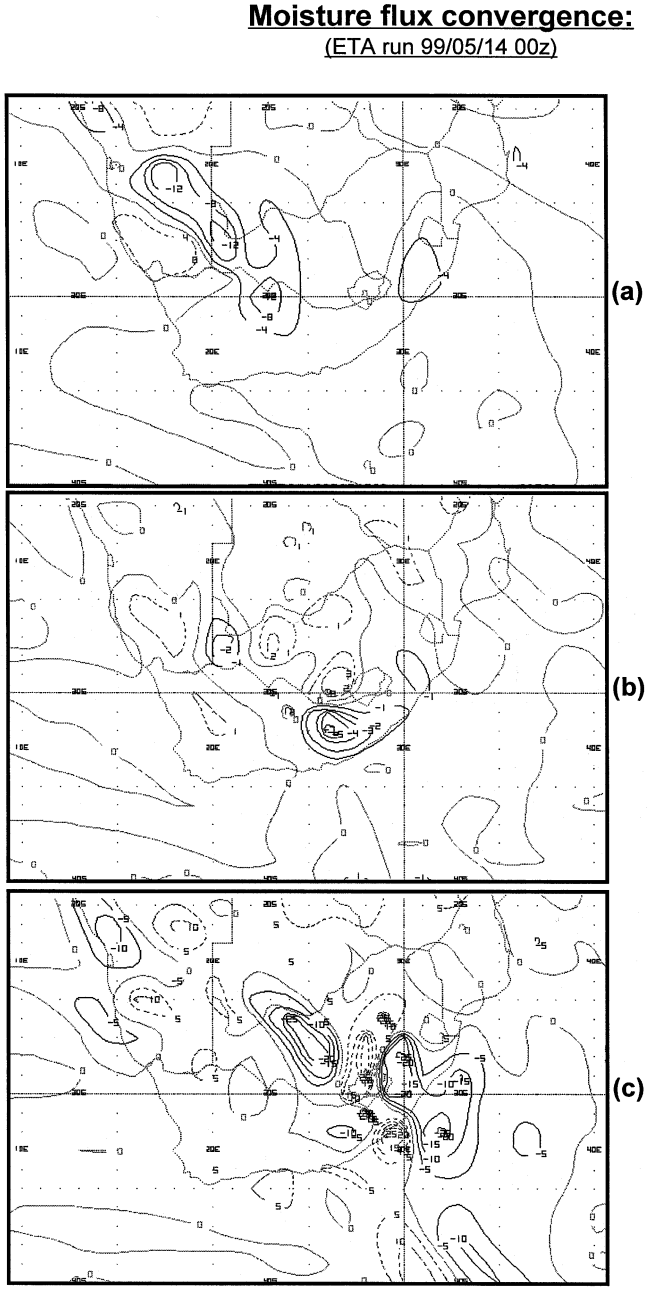

Figure 10

Moisture flux convergence (10^{-5} g·cm^{-2}·s^{-1}) from the Eta model's midnight run (99051400) for a) 12:00 UTC in the 310-314K layer, b) 18:00 UTC in the 302-306K layer and c) 24:00 UTC in the 302-306K layer

Condensation pressure difference

This variable gives an indication of the saturation level of the air at a certain level. The smaller the values, the closer to saturation. The values (mostly smaller than 100 hPa) indicate that the air was close to saturation throughout the time period (not shown) over the central parts of the country.

Volumetric moisture in the isentropic layer

This indicates the total moisture content of the isentropic layer, greater values indicate more moisture in the layer.
The bulk of the moisture at 12:00 UTC (Fig. 9a) was concentrated over Namibia extending into the northern Cape. By 18:00 UTC (Fig. 9b) the moisture had moved well into the central and northern interior, as well as into the eastern Cape with dry air persisting over Lesotho. Moisture diminished significantly over the west. At 24:00 UTC (Fig. 9c) drier air had taken over the western half of the country, while a band of moisture was evident from southern Botswana extending across the country over southern KwaZulu-Natal.

Moisture flux in the isentropic layer

This field illustrates graphically the transport of moisture as described in the previous paragraph.

Moisture flux convergence in the isentropic layer

Moisture flux convergence indicates where moisture is increasing locally. In conjunction with decreasing stability, it indicates where the greatest potential for convective development is focused.
At 12:00 UTC (Fig. 10a) moisture is converging (negative values) over the southern and central parts of the country with the maximum accumulation in a band over the Kalahari and northern Cape. By 18:00 UTC (Fig. 10b) the convergent area was focused over the eastern Cape with an area of divergence over the Free State, North-West Province and north-eastern parts of northern Cape. However, there was a marked reaccumulation of moisture over this area at 24:00 UTC (Fig. 10c), with strong divergence east of that.

Isentropic interpretation

At 12:00 UTC, decreased stability, vertical adiabatic motion, ample moisture were present, but these fields were not coincident at this time and no rain was reported during the period 1200 until 18:00 UTC.

At 18:00 UTC the following factors contributed to favourable rainfall conditions in the area where the first rainfall episode with lighter falls occurred (over the central interior):

- Relatively high isentropic mass (lower stability) in 302-306K
- Weak upward vertical adiabatic motion at 302K, but more pronounced at 306K
- Condensation pressure differences were low - close to saturation situation on 302K
- High volumetric moisture in the 302-306K layer

If there was moisture flux convergence as well, it would have rained harder, but moisture flux convergence fields indicated slight divergence in this area and therefore rainfall was only light.

At 24:00 UTC the following factors contributed to favourable rainfall conditions in the area where the second, heavier rainfall episode occurred (western half of the Free State, the eastern parts of the Northern Cape Province and the south-western parts of the North-West Province):

- Relatively high isentropic mass (lower stability) in 302-306K
- Regeneration of upward adiabatic motion at 302K and more significant upward motion at 306K
- Low condensation pressure difference values (close to saturation) on 302K
- Relatively high volumetric moisture values in 302-306K
- Moisture convergence on 302K
- Moisture transport into the area on 302K
- Moisture flux convergence in 302-306K layer.

With the added ingredient of moisture flux convergence to the already favourable factors before, rainfall totals were higher in this case. This rainfall event was most effective in the west of the rainfall region (central interior) and weakened as it moved through to the east, where only very light rain was reported over the southern parts of Gauteng.

Summary and conclusions

Isentropic analysis of model output fields adds a third dimension to air flow in the atmosphere. This concept is especially helpful in monitoring the movement or transport of moisture and therefore offers assistance in the prediction of precipitation. Although isentropic analysis is not meant to be a substitute for isobaric analysis, is can be a very helpful aid in making more accurate forecasts possible. Quoting Uccellini (1995): "*Given the advancements in the utilisation of the isentropic framework, the question no longer is IF the isentropic framework positively impacts analysis and forecasts; the question is now HOW to integrate this framework into the operational community at all levels of the forecast process*".

Recent studies on weather patterns over South Africa (De Coning, 1997; De Coning et al.,1998 and De Coning and Petersen, 1999) have shown that these concepts could also be used in our country. With the aid of PCGRIDDS (a PC-based Gridded Information Display and Diagnostic System) the interpolation to isentropic levels (levels of constant potential temperature, θ) is done by a few easy steps off the main menu. The isentropic variables described in this study were displayed by typing easy commands in PCGRIDDS. A practical manual (De Coning and Banitz, 1999) is available for all forecast offices around the country. Since the improvement of short-term weather forecasts will always be a priority in this country, it is believed that isentropic analysis can provide the forecaster with an additional way of looking at model output data which can open up new horizons.

Acknowledgments

The author would like to acknowledge the guidance with regard to the operational use of isentropic analysis for South African circumstances through case studies and PCGRIDDS received from Greg Forbes (Severe Weather Expert, The Weather Channel, Atlanta, USA) and Ralph Petersen (National Centre for Environmental Prediction, USA). The author is also indebted to Lucian Banitz who helped with the PCGRIDDS macro development and the isentropic manual for operational forecasters (De Coning and Banitz, 1999).

References

ANDERSON JL (1984) The use and interpretation of isentropic analyses. *NOAA Technical Memorandum NWS WR-188.* Scientific Services Division, National Weather Service Western Region, Salt Lake City, Utah.

BLECK R (1973) Numerical forecasting experiments based on the conservation of potential vorticity on isentropic surfaces. *J. Appl. Meteor.* **12** 737-752.

BYERS HR (1938) On the thermodynamic interpretation of isentropic charts. *Monthly Weather Rev.* **66** (3) 63-69.

CARLSON TN (1991) Airflow through mid-latitude synoptic scale disturbances. In: *Mid-latitude Weather Systems*, NY Harper-Collins Academic. 284-341.

DANIELSEN EF (1959) The laminar structure of the atmosphere and its relation to the concept of the tropopause. *Arch. Meteor. Geophys. Bioklim. Atol. Ser.* **11** 232-293.

DANIELSEN EF (1961) Trajectories: Isobaric and actual. *J. Meteor.* **18** 479-486.

DE CONING E (1997) Isentropic Analysis as a Forecasting Tool in South Africa. Unpublished Master's Thesis, Univ. of Pretoria.

DE CONING E and BANITZ L (1999) Now is the time to make the theta connection - Isentropic Analysis using PCGRIDDS. South African Weather Bureau Internal Training Manual for Operational Forecasters.

DE CONING E and PETERSEN R (1999) A case of severe convection in South Africa - Assessment of conventional numerical guidance using isentropic techniques. *Proc. 2nd Conf. on Isentropic Analysis and Forecasting*. Millersville, PA. 9-10 April .

DE CONING E, FORBES GS and POOLMAN E (1998) Heavy rain and flooding on 12-14 February 1996 over the summer rainfall regions of South Africa: Synoptic and isentropic analyses. *NWA Digest* **22** (3) 25-36.

HESS SL (1959) *Introduction to Theoretical Meteorology*. NY. Holt Reinhart and Windston.

KOROTKY J, MOORE JT and MARKET PS (1999) Evaluating adiabatic vertical motion. *Proc. 2nd Conf. on Isentropic Analysis and Forecasting*. Millersville, PA. 9-10 April.

MARKET PS and MOORE JT (1995) An isentropic perspective on elevated thunderstorms with heavy rainfall. *Proc. 1st Conf. on Isentropic Analysis and Forecasting*. Lancaster, PA, 31 March - 2 April.

MARKET PS, MOORE JT and SCOTT MR (1999) On calculating vertical motions in isentropic coordinates . *Proc. 2nd Conf. on Isentropic Analysis and forecasting.* Millersville, PA. 9-10 April .

MILLS GA and BAO-JUN W (1995) The Cuddle-creek flash flood - An example of synoptic scale forcing of a mesoscale event. *Austr. Met. Magazine* **44** 201-218.

MOORE JT (1992) Isentropic analysis and interpretation: Operational applications to synoptic and mesoscale forecasting problems. Internal publication of the Dept. of Earth and Atmos. Sci., St Louis Univ.

NAMIAS J (1938) Thunderstorm forecasting with the aid of isentropic analysis charts. *Bull. Am. Metereol. Soc.***19** 1-14.

NOLAN M and MOORE JT (1995) An isentropic analysis of a heavy snow event associated with weak cyclogenesis. *Proc. 1st Conf. on Isentropic Analysis and Forecasting*, Lancaster, PA. 31 March - 2 April.

OLIVER VJ and OLIVER MB (1951) Meteorological analysis in the middle latitudes. *Compendium of Meteorology.* Boston, MA, Am. Meteor. Soc. 715-727.

PETERSEN R and KOROTKY J (1999) Evaluating mass and moisture in an isentropic layer. *Proc. 2nd Conf. on Isentropic Analysis and Forecasting.* Millersville, PA. 9-10 April.

ROGERS RR and YAU MK (1989) *A Short Course in Cloud Physics* (3rd edn.) Edited by D Ter Haar. Pergamon Press, Canada. 293 pp.

ROSSBY CG, KEILY DP, OSMIN JWW and NAMIAS J (1937) Isentropic analysis. *Bull. Am. Meteor*. **18** 201-209.

UCCELLINI LW (1995) Isentropic analysis for meteorological applications. *Proc. 1st Conf. on Isentropic Analysis and Forecasting*, Lancaster, PA. 31 March- 2 April.

WILSON LJ (1985) *Isentropic Analysis - Operational Applications and Interpretation* (3rd edn.) Edited for Training Branch by James Percy. Atmospheric Environment Service, Canada. 35 pp.